# CHAPTER 2

# Information localization and verification of the firing states of an artillery gun

Maksym Maksymov
Pavlo Gultsov
Volodymyr Demydenko
Valentin Davydov

**Abstract**

This chapter investigates the problem of informational localization and verification of the states that characterize the lifecycle of an individual artillery shot. The study considers the sequential chain of physical processes occurring in the system "propellant charge – chamber – barrel – projectile – flight trajectory – impact with the surface". These processes form the basis for assessing the technical condition and operational efficiency of artillery systems.

A conceptual framework is developed for identifying measurable parameters associated with different stages of the shot process. The approach relies on the analysis of acoustic, thermodynamic, and optoelectronic phenomena accompanying the firing event. Particular attention is given to the diagnostic potential of the acoustic field generated by ballistic and muzzle waves.

A method for verifying the heat of explosion of the propellant charge is proposed. The method is based on determining the gross chemical formula of the propellant gases and performing a thermodynamic evaluation of the energy characteristics of the charge. This approach enables verification of the declared energetic parameters of propellant compositions.

An acoustic method for estimating the initial velocity of the projectile is presented. The method utilizes temporal characteristics of ballistic and muzzle waves recorded at remote measurement points and allows indirect assessment of the wear state of the barrel and chamber.

The chapter also introduces a method for evaluating the energetic efficiency of an artillery gun based on video-metric observation of projectile exit and the expansion of propellant gases. In addition, a technique for verifying the coordinates of

 DOI: 10.21303/978-9908-8450-1-2.ch2

projectile impact is proposed using acoustic measurements of the shot-generated wave field along the projectile trajectory.

The presented models and methods provide a basis for partial verification of different stages of the artillery shot process and may serve as elements of integrated automated systems for monitoring the technical condition and operational parameters of artillery weapons.

**Keywords**

Artillery shot diagnostics, acoustic field of a shot, ballistic and muzzle waves, propellant charge energetics, artillery gun efficiency, projectile trajectory verification.

## 2.1 Introduction

Modern artillery operations are characterized by increasingly high demands on precision, rapid response, and verification of firing results under dynamic conditions. In contemporary combat and training scenarios, the ability to accurately assess the technical state of artillery systems immediately after a shot is essential for both operational efficiency and safety. The complex interactions between the propellant charge, chamber, barrel, and projectile, along with the influence of environmental factors, require the use of integrated measurement and diagnostic methods to monitor the firing process in real time [1, 2].

Recent studies demonstrate that combining heterogeneous physical measurements – acoustic, thermodynamic, and optoelectronic – can provide a reliable basis for evaluating the performance and condition of artillery systems [3, 4]. Acoustic signals generated during firing, such as ballistic and muzzle waves, carry information about the projectile's initial velocity, barrel wear, and the energetic characteristics of the propellant charge. Meanwhile, high-speed videometric recordings allow observation of projectile exit dynamics and the expansion of propellant gases, which can be used to assess energetic efficiency [5, 6].

Methodological approaches originally developed in related fields – such as the modeling of combustion processes, pyrolysis, and energy transformations in reactive systems – can be adapted for interpreting measurement signals obtained during firing [7, 8]. For instance, analytical solutions of differential equations, parameter identification techniques, and library-based process models provide a flexible framework for describing nonlinear dynamic phenomena in artillery systems. These approaches support the development of partial verification methods for individual stages of a shot, from propellant ignition to projectile impact.

At the same time, operational considerations in artillery units, including rapid repositioning, variation in ammunition properties, and environmental disturbances, necessitate methods that are both accurate and deployable under real conditions [9]. The integration of measurement data with computational methods enables real-time assessment of firing states, minimizing the time between successive shots while maintaining reliability in the determination of energetic and kinematic parameters.

Within this context, the present chapter focuses on the development of diagnostic and verification methods for artillery shots based on the combined analysis of acoustic fields, videometric observations, and thermodynamic measurements. Particular attention is given to the identification of measurable parameters at each stage of the firing process, methods for verifying the heat of explosion of propellant charges, localizing initial projectile velocity, evaluating energetic efficiency, and verifying the coordinates of projectile impact [10]. By presenting a coherent framework for integrating these methods, the chapter lays the foundation for automated monitoring systems capable of supporting both operational decision-making and scientific research in artillery performance assessment.

## 2.2 General provisions

The firing process of an artillery gun can reasonably be considered as a multifactor dynamic system operating through a sequential transition of states "propellant charge – chamber – barrel – projectile – trajectory – impact with the surface". Such a transition may be formalized in the form of a directed graph of states, in which each link is characterized by a set of thermodynamic, mechanical, and ballistic parameters.

The stochastic nature of variations in propellant properties, barrel wear, projectile mass, and meteorological conditions necessitates the information-based localization of the current system state in real time. In modern automated fire-control systems, verification is performed within a single computational cycle without waiting for the results of the previous shot. This approach makes it possible to minimize time losses and to increase the generalized firing efficiency criterion by nearly five times compared with the classical adjustment-firing scheme.

An analysis of open sources indicates that information localization methods can be systematized according to the physical nature of the measured field.

Photoelectric and videometric methods make it possible to determine projectile velocity and coordinates based on high-speed imaging results [11, 12]. Their advantage lies in high measurement accuracy; however, their effectiveness depends on atmospheric observation conditions.

Radar-based methods, particularly Doppler systems, provide measurements of motion parameters along the initial and intermediate segments of the trajectory [13, 14]. These methods are less sensitive to visibility conditions but require more complex hardware implementation.

Acoustic methods are based on the registration of muzzle and ballistic waves and make it possible both to localize firing positions and to determine projectile velocity [2, 3, 15–17]. Their advantage lies in the relative simplicity of deployment, while the informational content is ensured through the analysis of the temporal and spectral characteristics of the signal.

A separate area is represented by tomographic and thermodynamic methods for monitoring ammunition quality throughout its life cycle [18]. Changes in the physicochemical properties of propellants during long-term storage affect the heat of explosion and, consequently, the initial projectile velocity and the energetic efficiency of the shot. The concept of an electronic ammunition passport appears promising under peacetime conditions; however, under conditions of intensive combat use, methods of operational verification that are independent of production history are more appropriate.

Thus, the information localization of firing states should be based on the direct measurement of physical parameters that determine the energetic and kinematic outcome. The following subsections examine the method for verifying the heat of explosion of the propellant charge and the method for localizing the initial projectile velocity based on acoustic fields as key components of an integrated monitoring system.

At the same time, it should be emphasized that the approaches to information localization based on acoustic, radar, and optoelectronic measurements considered above represent a generalization of known methods described in the literature. The subsequent subsections present the authors' original contributions, including the verification method for the heat of explosion of the propellant charge, the acoustic method for localizing the initial projectile velocity, the videometric method for determining energetic efficiency, and the method for verifying the projectile impact coordinates. These methods are proposed as a unified framework for integrated diagnostics of artillery firing states.

### 2.3 Method for determining the heat of explosion of the propellant charge as a tool for verifying its state

To confirm the compliance of the energetic characteristics of the propellant charge with the established requirements, an automated system for determining

the heat of explosion is employed together with a corresponding computational-experimental verification method, the schematic diagram of which is shown in **Fig. 2.1**.

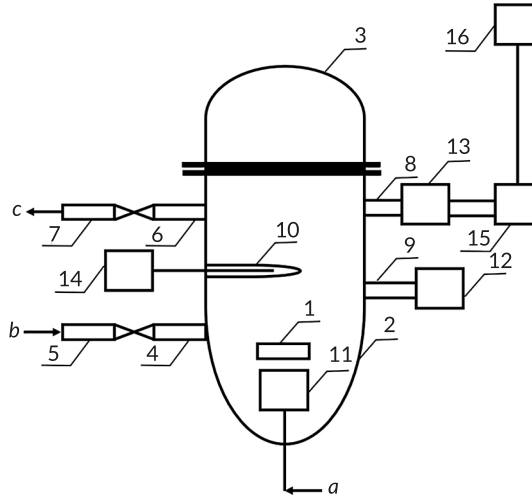


**Fig. 2.1** Automated system for determining the heat of explosion of an artillery propellant charge for verification of its quality: *a* – the voltage supply line; *b* – the line supplying inert gas to the tank; *c* – the line for inert gas removal; 1 – the propellant charge sample; 2 – the cylindrical tank; 3 – the flanged cover; 4 – the inlet fitting; 5 – the shut-off equipment; 6 – the outlet fitting; 7 – the shut-off equipment; 8 – the fitting; 9 – the fitting; 10 – the sleeve; 11 – the electric igniter; 12 – the pressure gauge; 13 – the gas pressure regulator; 14 – the thermocouple via the indication device; 15 – the composition of the combustible gas; 16 – personal computer with appropriate software

The automated system for determining the heat of explosion of an artillery propellant charge for quality verification includes a cylindrical tank (2) with an internally heat-insulated surface designed for burning a sample of the propellant charge and collecting the generated propellant gases. The outlet of the gas pressure regulator (13) is connected to the inlet of the installation for determining the composition of the combustible gas during combustion (15), the output of which is connected to a personal computer with appropriate software (16).

In the upper part of the tank, a hermetically sealed flanged cover (3) with thermal insulation is installed; in the lower part, an electric igniter (11) is mounted, while a sleeve (10) for a thermocouple with a temperature indication device (14) is located on the side wall.

An inlet fitting (4) with shut-off equipment for purging with inert gas (5) and an outlet fitting (6) with corresponding shut-off equipment (7) are mounted on the side wall of the tank. In addition, a fitting (9) is provided for connecting a pressure gauge (12), as well as a fitting (8) connected to the gas pressure regulator (13).

**Fig. 2.1** additionally designates the propellant charge sample (1), the voltage supply line ("*a*"), the lines supplying inert gas to the tank ("*b*"), and the line for its removal ("*c*").

The installation for determining the composition of combustible gas during its combustion (15) is known from the literature [19]. It includes an energy device with a burner, a system for supplying combustible gas and air with regulating equipment, pipelines for gas and air sampling, flowmeters and flow sensors, a control unit, and a testing device. The burner is connected to the pipelines supplying combustible gas and air. Corresponding flow sensors and regulating equipment are installed on the pipelines supplying combustible gas and air. The supply pipelines are connected to the sampling pipelines, which are routed to the testing device. The control unit interacts with the regulating equipment, flow sensors, flowmeters, and a thermocouple installed in the combustion chamber of the testing device, ensuring control of the combustion regimes.

The testing device contains a cylindrical combustion chamber with coaxially arranged cylinders between which gaps are formed for the passage of air. The chamber is equipped with pipes for supplying combustible gas and air, fitted with temperature measurement devices. Inside the chamber, a thermocouple is installed to monitor the combustion temperature regime.

The proposed method is implemented in the following sequence.

At the first stage, a batch of identical propellant charges of artillery rounds is delivered for verification, for which confirmation of the heat of explosion obtained at the loading plant and documented by the packing arsenal is available. A sample of the propellant charge (1) is taken from a randomly selected round and placed in the cylindrical tank (2) of the system, after which the tank is hermetically sealed with the flanged cover (3).

At the second stage, a specified constant pressure is set in the throttling regulator of the gas pressure regulator (13) for the subsequent throttling of the propellant gas.

The third stage involves removing air from the tank by purging it with inert gas, which is supplied through the inlet fitting (4) with shut-off equipment (5) and discharged through the outlet fitting (6) with corresponding equipment (7).

At the fourth stage, the pressure of the inert gas is monitored by the pressure gauge (12) connected through the fitting (9). After atmospheric pressure has been established, the shut-off equipment (5) and (7) are closed and voltage is supplied to the electric igniter (11), igniting the propellant charge sample (1).

At the fifth stage, the generated propellant gases are directed from the tank (2) through the fitting (8) and the gas pressure regulator (13) to the installation for determining the composition of the combustible gas (15).

At the sixth stage, the propellant gas is burned in an air atmosphere in the installation (15), and the gross formula of the gas formed during the combustion of the propellant charge sample (1) is determined.

At the seventh stage, the obtained gross formula is transmitted to a personal computer with appropriate software. Additionally, the temperature value obtained from the thermocouple via the indication device (14) installed in the sleeve (10) on the wall of the tank (2), the pressure value set by the gas pressure regulator (13), and the declared heat of explosion of the propellant charge are entered.

At the eighth stage, using the computer software, a thermodynamic calculation of the heat of explosion of the propellant charge sample is performed based on the determined gross formula of the propellant gas and the measured process parameters. The obtained value is compared with the declared one, taking into account measurement and calculation errors. If the values coincide within the permissible error, a conclusion is made regarding the positive verification of the heat-of-explosion property of the artillery propellant charge; otherwise, the verification result is considered negative.

The initial data for determining the heat of explosion of the propellant charge are presented in **Table 2.1**. In Example 1, calculated and experimental data are presented concerning the application of the system and the method at site *B*, where assembled rounds of the same type in the amount of *N* units were delivered from arsenal *WW*. For the study, one of the delivered rounds was randomly selected. A sample (1) of the propellant charge was taken from the selected round for the measurement experiment. The sample (1) was placed in the cylindrical tank (2) of the heat-of-explosion determination system.

Similarly, in Example 2, calculated and experimental data are presented concerning the application of the system and the method at site *C*, where assembled rounds of the same type in the amount of *M* units were delivered from arsenal *WV*. An analogous procedure of round selection and sample preparation was performed for Example 2. In both cases, the experiment was carried out and a result was obtained.

From the presented data, the following conclusions can be drawn. The declared heat of explosion of the artillery propellant charge in Example 1 is 950 kJ/kg, and in Example 2 it is 945 kJ/kg (see item 7 of **Table 2.1**). The total relative error of measurements and calculations is 1.5% (see item 6 of **Table 2.1**) and is adopted as the criterion for comparing the declared and calculated values of the heat of explosion. The gross formula of the propellant gas obtained experimentally was determined as $C_1H_{1.44}N_{0.37}O_{1.57}$ for Example 1 and $C_1H_{1.43}N_{0.32}O_{1.56}$ for Example 2 (item 2 of **Table 2.1**).

**Table 2.1 Indicators of the properties of quantities obtained during the verification of the heat of explosion of the propellant charge of an artillery round**

| No. | Name of indicator, unit of measurement | Values of indicators in the experiments | |
|---|---|---|---|
| | | Example No. 1 | Example No. 2 |
| 1 | Pressure of the propellant gas during throttling set on the gas pressure regulator, Pa | $1.1 \cdot 10^5$ | $1.1 \cdot 10^5$ |
| 2 | Gross formula of the propellant gas | $C_1H_{1.44}N_{0.37}O_{1.57}$ | $C_1H_{1.43}N_{0.32}O_{1.56}$ |
| 3 | Temperature value recorded by the thermocouple, K | 2800 | 2300 |
| 4 | Pressure value in the cylindrical tank after the formation of the propellant gas, Pa | $5.1\ 10^5$ | $4.8\ 10^5$ |
| 5 | Total relative measurement and calculation error, % | 1.5 | 1.5 |
| 6 | Declared heat of explosion of the propellant charge of the artillery round, kJ/kg | 950 | 945 |
| 7 | Calculated heat of explosion of the propellant charge of the artillery round, kJ/kg | 958 | 890 |
| 8 | Value of the relative experimental error, % | 0.84 | 5.82 |
| 9 | Comparison of the errors of the declared and calculated heat of explosion values | $0.84 < 1.5$ | $5.82 > 1.5$ |
| 10 | Conclusion on the comparison of declared and calculated heat of explosion | Equality within the limits of experimental error | No equality within the limits of experimental error |
| 11 | Verification result | Positive | Negative |

Based on the determined gross formula of the propellant gas and the measured process parameters, the heat of explosion of the propellant charge was calculated, amounting to 958 kJ/kg for Example 1 and 890 kJ/kg for Example 2 (item 7 of **Table 2.1**). The relative experimental errors were determined as 0.84% for Example 1 and 5.82% for Example 2 (item 9 of **Table 2.1**).

An analysis of the obtained results shows that the calculated value of the heat of explosion is primarily influenced by the determined gross formula of the propellant gas and the measured temperature, which define the thermodynamic state of the combustion products. Pressure plays a secondary role under the adopted calculation scheme, while the total measurement and calculation error establishes the admissible range for comparing the calculated and declared values. Therefore, deviations exceeding the specified error threshold may indicate changes in the physicochemical properties of the propellant charge rather than measurement uncertainty.

An analysis of the results presented in **Table 2.1** shows that for Example 1 the verification result is positive, whereas for Example 2 it is negative.

The data obtained from Examples 1 and 2 demonstrate the practical feasibility of verifying the propellant charge of an artillery round using the proposed system and method.

## 2.4 Method for localizing the initial projectile velocity during the generation of acoustic fields of the shot

There are studies in the field of information technologies that have demonstrated the possibility of performing automated diagnostics of the "barrel-chamber" system state based on the velocity of the projectile exiting the barrel [2, 3, 15–17, 20].

The method is illustrated by the equipment arrangement shown in **Fig. 2.2**. In **Fig. 2.2**, the following are indicated: 1 – gun, 2 – microphone or microphones, 3 – air temperature sensor at the gun, 4 – air pressure sensor at the gun, 5 – air humidity sensor near the gun, 6 – wind direction and speed sensor, 7 – air temperature sensor near the microphone or microphones (2), 8 – air pressure sensor near the microphone or microphones (2), 9 – air humidity sensor near the microphone or microphones (2), 10 – wind direction and speed sensor near the microphone or microphones (2), 11 – ballistic wave, 12 – muzzle wave, $S_1$ – distance from the gun to the microphone or microphones (2) along the firing direction, $S_2$ – distance from the microphone or microphones (2) to the location of the ballistic wave (11) along the firing direction at the moment the microphone or microphones (2) registered the muzzle wave (12), $S_3$ – distance from the gun to the location of the muzzle wave (12) at time $t_{bal}$ (14), when the ballistic wave (11) was registered by the microphone or microphones (2) at distance $S_1$.

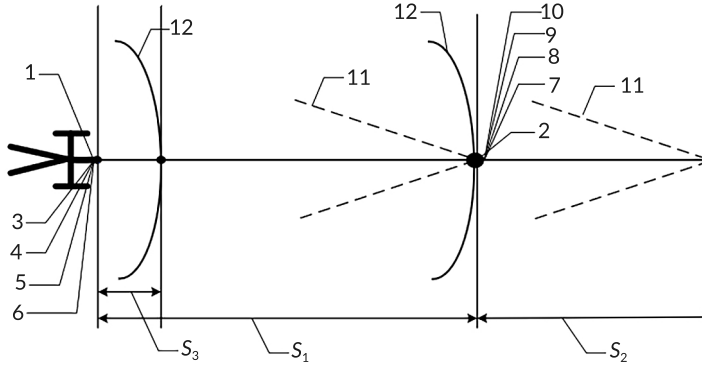


**Fig. 2.2** Diagram of the gun and measurement equipment arrangement

In **Fig. 2.3**, the following are shown: 13 – moment of muzzle wave registration $t_{muz}$, 14 – moment of ballistic wave registration $t_{bal}$, 15 – time interval recorded by the microphone or microphones (2) between the passage of the ballistic wave $t_{bal}$ and the muzzle wave $t_{muz}$.

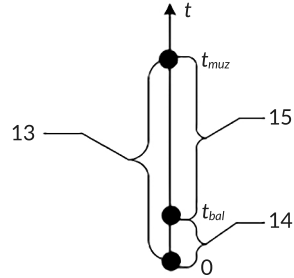


**Fig. 2.3** Time diagram of wave registration $t_{muz}$, $t_{bal}$ at the microphone location

The method is implemented in the following sequence:

**Step 1**. A gun (1) with a barrel and chamber is placed at the firing position and subjected to inspection. The degree of gun wear is preliminarily assessed by the total number of rounds fired from the gun. The gun is then loaded with a specific projectile and a corresponding propellant charge.

**Step 2**. A microphone or microphones (2) are placed along the line of fire at a distance of 50–500 meters from the gun (1). The microphone or microphones (2) are positioned along the firing direction for the registration of the ballistic (11) and muzzle (12) waves. Measurements of atmospheric parameters near the gun are carried out using temperature (3), pressure (4), humidity (5), and wind speed and direction (6) sensors. Similar measurements are performed at the location of the microphone using sensors (7–10). Based on the obtained values, a correction to the propagation velocity of the muzzle wave under the existing atmospheric conditions is determined.

**Step 3**. A shot is fired from the gun (1) in the firing direction.

**Step 4**. Using the microphones (2), the ballistic wave (11) is first registered. At this moment in time $t_{bal}$ (14), the muzzle wave (12) is located at a distance $S_3$ from the gun (1). After a time $t_{muz}$ (13), the microphones (2) register the muzzle wave (12) from the shot; at this moment the ballistic wave (11) is located at the total distance $S_1 + S_2$ from the gun (1).

**Step 5**. From the obtained temporal signal patterns, the amplitude and duration of the ballistic wave signal (11) are determined, as well as the amplitude and the

duration of the first half-period of the muzzle wave (12) at the microphone location (2) at a distance $S_1$ from the gun (1).

**Step 6**. The signals from the microphone or microphones (2) are transmitted to an analog-to-digital converter and then to a computer, where the signals are transformed into the spectral domain by computing the Fourier transform. In the spectral domain, the power spectral density (or simply the spectrum) is obtained, characterizing the distribution of signal energy over different frequencies.

**Step 7**. For the obtained spectra, the width at the level of 0.707 is determined for the ballistic wave signal (11), and the central frequency (frequency of the maximum) is determined for the muzzle wave (12).

**Step 8**. The travel time of the muzzle wave $t_{muz}$ (13) from the gun (1) to the microphones (2) is determined from the measured distance from the gun (1) to the microphones (2), $S_1$, and the calculated propagation velocity of the muzzle wave (12).

**Step 9**. The travel time of the ballistic wave $t_{bal}$ (14) from the gun (1) to the microphones (2) is determined as the difference between the travel time of the muzzle wave $t_{muz}$ (13) to the microphones (2) and the time interval (15) recorded during the passage of the ballistic wave (11).

**Step 10**. The velocity of the ballistic wave (11) (which corresponds to the instantaneous projectile velocity) is determined using the time $t_{bal}$ (14) at which it is registered by the microphones (2) at a distance $S_1$ from the gun (1).

**Step 11**. The calculated actual initial projectile velocity – 558.2 m/s (item 17 in **Table 2.2**) – is compared with the calculated nominal initial projectile velocity – 560 m/s (see item 16 in **Table 2.2**), and a conclusion is drawn regarding the degree of wear of the barrel and chamber based on the change in projectile velocity.

After that, a second shot is fired from the same gun (1) at the firing position, and all the operations described above are repeated.

**Table 2.2** shows that the first gun (item 2 in **Table 2.2**) does not exhibit a significant difference between the calculated actual projectile velocities – 558.2 m/s and 556.9 m/s – and the calculated nominal initial velocity of 560 m/s.

The difference between the calculated nominal initial projectile velocity and the calculated actual initial projectile velocity is 0.32% and 0.55%, respectively.

The wear of the first gun is insignificant (**Table 2.2**), since the difference does not exceed the permissible threshold of 8–10%.

This conclusion is based on the proposed method, in which the criterion for assessing barrel and chamber wear is primarily determined by the relative deviation of the calculated actual initial projectile velocity from the nominal (tabulated) value. At the same time, the recorded acoustic parameters (signal amplitudes, durations, and spectral characteristics) are used as auxiliary informative features

that ensure the reliability of velocity determination. Thus, the final conclusion about the degree of wear is formed according to a combined criterion, where the key quantitative indicator is the velocity deviation, supported by the stability of the acoustic signal parameters.

**Table 2.2 Indicators of barrel and chamber wear of the artillery gun**

| No. | Name of indicator, unit of measurement | Value of the indicator for the gun | | | |
|---|---|---|---|---|---|
| | | First | | Second | |
| 1 | Experiment number | 1 | 2 | 3 | 4 |
| 2 | Total number of shots fired from the gun | 91 | | 1968 | |
| 3 | Shot number from the gun | 1 | 2 | 1 | 2 |
| 4 | Distance from the gun to the measuring microphone, m | 300 | | | |
| 5 | Tabulated firing range according to the sight setting, m | 9000 | | | |
| 6 | Total correction for meteorological conditions, m | –137 | –157 | –215 | –215 |
| 7 | Ballistic corrections, m | +12 | | | |
| 8 | Calculated firing range, m | 8875 | 8855 | 8797 | 8797 |
| 9 | Actual firing range determined by the rangefinder, m | 9165 | 9082 | 8665 | 8671 |
| 10 | Amplitude of the ballistic wave, Pa | 380 | | 240 | |
| 11 | Duration of the ballistic wave signal, ms | 4.8 | | 4.1 | |
| 12 | Amplitude of the muzzle wave, Pa | 140 | | 90 | |
| 13 | Duration of the first half-period of the muzzle wave, ms | 22 | | 14 | |
| 14 | Spectrum width at the 0.707 level of the ballistic wave signal, Hz | 180 | | 250 | |
| 15 | Central frequency (frequency of the maximum) of the muzzle wave signal spectrum, Hz | 12 | | 16 | |
| 16 | Calculated initial projectile velocity, m/s | 560 | | | |
| 17 | Calculated actual initial projectile velocity, m/s | 558.2 | 556.9 | 504.2 | 504.5 |

Subsequently, a second gun is placed at the firing position and all the operations listed above are performed. The obtained data are entered into the table. For the second gun (**Table 2.2**), the calculated actual projectile velocities are 504.2 m/s and 504.5 m/s, while the calculated nominal initial projectile velocity is 560 m/s, which corresponds to deviations of 9.96% and 9.91%, respectively.

Thus, as a result of performing the specified sequence of operations for two guns (item 2 of **Table 2.2**), each of which fired two shots (item 3 of **Table 2.2**), a set

of parameters was obtained that characterizes disturbances of the atmospheric environment caused by the shot and calculated from the registration times of the muzzle wave $t_{muz}$ (13) and the ballistic wave $t_{bal}$ (14). On this basis, a conclusion was drawn regarding the level of wear of the barrel bore and the chamber of each gun (items 10–17 of **Table 2.2**). The wear of the second gun is significant, since the calculated actual projectile velocities in the two shots are 9.96% and 9.91% lower than the calculated nominal initial velocity, which is confirmed by the data presented in items 5, 8, and 9 of **Table 2.2**.

The obtained results confirm the possibility of practical application of the method for assessing the wear of the barrel bore and the chamber. Previously, it was considered that rifled barrels of an artillery gun are unsuitable for further use if the total loss of the projectile's initial velocity due to barrel wear reaches 10% or more of the tabulated value.

### 2.5 Method for determining the energy efficiency of an artillery gun

Studies in the field of automated control systems have demonstrated the possibility of automated diagnostics of the state of the "propellant charge – chamber – barrel – shot" system based on the projectile velocity at the moment it exits the barrel bore and on the parameters of the muzzle emission [1, 5, 21, 22].

The method is aimed at determining the energy efficiency of an artillery gun, which makes it possible to increase the reliability of assessing its current condition. The method is explained by a specific arrangement of equipment shown in **Fig. 2.4–2.6**.

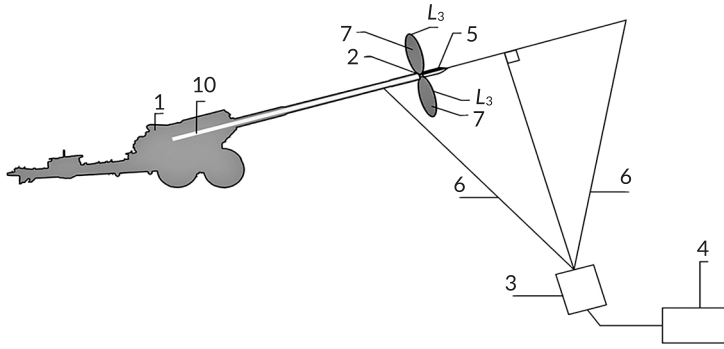


**Fig. 2.4** Equipment layout diagram

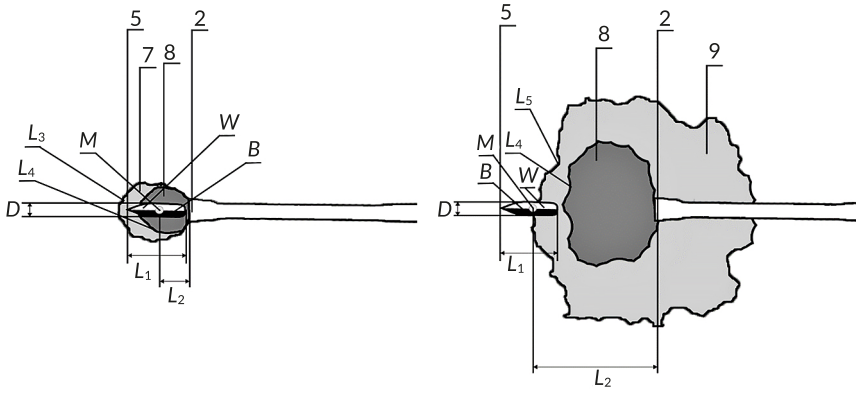


**Fig. 2.5** Diagram of two frames displaying fields that register temperature and pressure after the projectile exits the barrel bore (left – the current *i*-th frame of the video stream showing the moment the projectile leaves the muzzle of the gun barrel; right – the current *k*-th frame of the video stream showing the moment of the maximum volume of the flame of burned propellant gases during their expansion to atmospheric pressure)

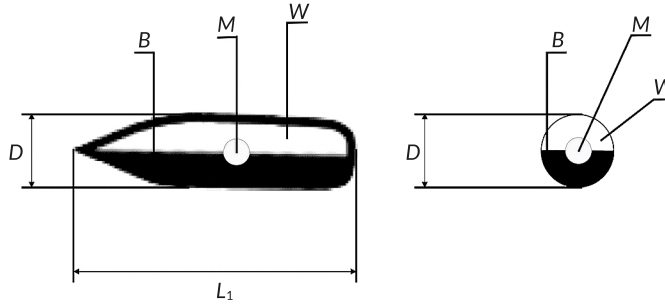


**Fig. 2.6** Diagram of binary coloring of the projectile

Artillery gun – 1; muzzle of the gun barrel bore – 2; digital high-frequency wide-angle video camera operating in the visible and infrared spectrum – 3; personal computer with processing software package – 4; projectile used for firing – 5; boundary of the camera field of view – 6; projection of the surface of unburned propellant gases of increased pressure – 7; projection of the surface of the flame of burned propellant gases – 8; projection of the surface of propellant gases expanded to atmospheric pressure and forming the acoustic muzzle wave – 9; internal volume of the barrel tube – 10; projectile caliber diameter – *D*; center of mass of the projectile – *M*; white field of

the binary-colored projectile – $W$; black field of the binary-colored projectile – $B$; projectile length – $L_1$; distance between the center of mass of the projectile (5) and the muzzle of the gun barrel bore – $L_2$; curved line representing the boundary between the projection of the surface of unburned propellant gases with pressure higher than atmospheric, forming the shock muzzle wave, and the atmosphere – $L_3$; curved line representing the boundary between the projection of the surface of the flame of burned propellant gases with pressure higher than atmospheric and the unburned propellant gases with pressure higher than atmospheric – $L_4$; curved line representing the boundary between the projection of the surface of the flame of burned propellant gases with pressure higher than atmospheric and the atmosphere – $L_5$; volume occupied by high-pressure propellant gases at the moment when the projectile (5) has passed the muzzle of the gun barrel bore (2) (internal volume of the barrel tube (10)) – $V$.

The method for determining the energy efficiency of an artillery gun is implemented in the following sequence:

**Step 1**. At the firing position, the artillery gun (1) is positioned so that the muzzle of the gun barrel bore (2) is perpendicular to the line along which the digital high-frequency wide-angle video camera (3) is placed, the latter being connected to a personal computer with a processing software package (4).

The position of the camera relative to the gun is not of fundamental importance.

**Step 2**. The projectile (5) prepared for firing is painted in two colors, white and black; the boundary line between the colors passes through the projectile nose along the generatrix of its contour (**Fig. 2.6**).

**Step 3**. The video camera (3) is activated, a shot is fired with the binary-colored projectile (5), recording is performed in the visible and infrared spectra, and the digital video stream is transmitted in real time to the personal computer with the processing software package (4).

**Step 4**. After the projectile (5) passes through the camera recording boundary (6), recording is stopped and the video camera (3) is switched off.

**Step 5**. Using the software package (4), the digital video stream is processed and converted into a sequence of frames.

**Step 6**. The frames are analyzed to detect the projectile, and an array of frames is formed from the moment it exits the muzzle of the barrel bore (2) to the moment it leaves the recording boundary (6).

**Step 7**. In the personal computer with the processing software package (4), for each time frame:

– the center of mass of the projectile $M$ is determined;

– at point $M$, the geometric scaling coefficient is determined using the a priori known projectile characteristics (diameter and length) in each time frame;

– the linear distance between the center of mass of the projectile (5) and the muzzle of the gun barrel bore is determined from the image of the barrel muzzle point (2) to point *M* of the projectile image (5), taking into account the geometric scaling coefficient;

– the instantaneous linear velocity of the projectile (5), *v*, is determined;

– the statistically reliable initial linear velocity of the projectile (5), $v_{start}$, is determined from the first time frames;

– the current color of the binary coloring of the projectile (5) (*W* or *B*) with the corresponding time is determined, and a temporal binary sequence is formed;

– from the temporal binary sequence, the number of rotations of the projectile (5) per unit time or the angular velocity $w_{start}$ of the projectile (5) is determined;

– the length of the curved line $L_3$, representing the boundary between the projection of the surface of unburned propellant gases and the atmosphere, is determined;

– the length of the curved line $L_4$, representing the boundary between the projection of the surface of the flame of burned propellant gases and the unburned propellant gases, is determined;

– from the constructed temporal series of lengths and areas, the gradients of pressure variation are determined; the absence of a pressure gradient indicates the formation of the curved line representing the boundary between the projection of the surface of the flame of burned propellant gases and the atmosphere (line $L_5$).

**Step 8.** Using the personal computer with the processing software suite (4), for each *i*-th time frame, the volume of propellant gases $V_{PG_i}$, the temperature of propellant gases $T_{PG_i}$ measured by the video camera (3), and the pressure of propellant gases $P_{PG_i}$ at the front of the muzzle blast wave are determined. Based on these values, the functional dependence $P(V) = f(V)$ is established.

**Step 9.** The volume of burnt propellant gases $V^*$ at atmospheric pressure is determined along curve $L_5$ – the boundary between the projection of the surface of burnt propellant gases at pressure above atmospheric and the atmosphere – corresponding to the pressure gradient generated by the shot.

**Step 10.** The following energies are determined for the projectile (5):

Kinetic energy along the trajectory: the projectile of mass *m* has

$$E_{kin} = \frac{1}{2} m v_{start}^2,$$

measured from the muzzle of the gun barrel (2).

Rotational energy

$$E_{rot} = \frac{1}{2}\left(\frac{D}{2}\right)^2 m w_{start}^2.$$

Work of expanding gases

$$E_g = \int P(V)\mathrm{d}V,$$

where $V$ – the volume of high-pressure propellant gases at the moment the projectile passes through the muzzle (internal barrel volume – 10), and $V^*$ – the volume of burnt propellant gases at atmospheric pressure.

The energetic efficiency of the artillery gun is then calculated as

$$eff = \frac{E_{kin} + E_{rot} + E_g}{E_{charge}},$$

where $E_{charge} = m_c Q_{expl}$ – the energy of the propellant charge used for firing, with $m_c$ the charge mass and $Q_{expl}$ the specific energy of the charge.

**Table 2.3** presents the determination of the geometric dimensions of curve $L_3$ and the projections of the propellant gas surfaces, as well as the volume of gas $V_{PG_i}$ that burns out, from the moment the projectile separates from the muzzle of the gun barrel until 100 ms, obtained through digital processing of the video stream captured by a high-speed wide-angle digital camera (2000 fps) in the visible and infrared spectra.

**Table 2.3 Determination of geometric dimensions of curve $L_3$**

| Number of the *i*-th video frame | Recording time, s | Length of the curve line $L_3$, m | Area of the surface projection 9, m$^2$ | Volume of propellant gases, $V_{PG_i}$, m$^3$ |
|---|---|---|---|---|
| 002 | 0.001 | 2.79 | 0.39 | 1.2 |
| 010 | 0.005 | 13.74 | 9.65 | 144.4 |
| 020 | 0.010 | 15.47 | 12.23 | 206.1 |
| 049 | 0.020 | 16.88 | 14.56 | 267.8 |
| 060 | 0.030 | 17.61 | 15.84 | 303.9 |
| 080 | 0.040 | 18.09 | 16.72 | 329.5 |
| 100 | 0.050 | 18.45 | 17.38 | 349.4 |
| 120 | 0.060 | 18.73 | 17.92 | 365.6 |
| 140 | 0.070 | 18.96 | 18.36 | 379.3 |
| 160 | 0.080 | 19.16 | 18.74 | 391.2 |
| 180 | 0.090 | 19.33 | 19.08 | 401.7 |
| 200 | 0.100 | 19.48 | 19.37 | 411.1 |

**Table 2.4** presents the determination of the temperature and the overpressure of the burnt propellant gases above atmospheric pressure from the moment the projectile separates from the muzzle of the gun barrel until 100 ms. These values are obtained by processing the video stream recorded by a high-speed wide-angle digital video camera (2000 fps) with data acquisition in the visible and infrared spectral ranges.

**Table 2.4 Determination of the temperature and overpressure of propellant gases above atmospheric pressure**

| Number of the *i*-th video frame | Recording time, s | Gas temperature $T_{PG_i}$, K | Calculated overpressure of propellant gases, $P_{PG_i}$, Pa |
|---|---|---|---|
| 002 | 0.001 | 303 | 66273 |
| 010 | 0.005 | 486 | 1010 |
| 020 | 0.010 | 669 | 973 |
| 049 | 0.020 | 829 | 928 |
| 060 | 0.030 | 832 | 821 |
| 080 | 0.040 | 765 | 696 |
| 100 | 0.050 | 673 | 578 |
| 120 | 0.060 | 580 | 476 |
| 140 | 0.070 | 497 | 393 |
| 160 | 0.080 | 428 | 328 |
| 180 | 0.090 | 372 | 277 |
| 200 | 0.100 | 328 | 239 |

Based on the presented data, the energetic efficiency of the artillery gun is *eff* = 0.31 (see item 17 in **Table 2.5**). This value corresponds to the typical range for artillery systems of this class, where a significant part of the energy of the propellant charge is dissipated through thermal losses, gas expansion, and acoustic emission. At the same time, a decrease in this value relative to expected levels may indicate increased energy losses associated with barrel wear, incomplete combustion of the propellant charge, or deviations in the internal ballistic process. Therefore, the energetic efficiency parameter can be considered as an integral diagnostic indicator of the technical state of the gun.

If any term in the numerator (items 10, 11, 13 in **Table 2.5**) or in the denominator (item 16 in **Table 2.5**) changes, the value of *eff* also changes. This indicates that

the current shot differs from the previous ones and should not be taken into account, which makes it possible to reduce the time required for gun sighting.

**Table 2.5 Determination of the energetic efficiency of the artillery gun**

| No. | Name of the parameter, unit of measurement | Calculated value |
|---|---|---|
| 1 | Projectile mass, $m$, kg | 46 |
| 2 | Projectile diameter, $D$, m | 0.152 |
| 3 | Analyzed video frames | 2, 3, 4, 5, 6, 7, 8, 9, 10 |
| 4 | Time interval, $\tau$, ms | 4 |
| 5 | Distance traveled by the projectile, $L_2$, m | 3.7 |
| 6 | Average initial linear velocity of the projectile, $v_{start}$, m/s | 925 |
| 7 | Number of revolutions during the time interval $\tau$ | 2.6 |
| 8 | Angular velocity of the projectile, $w_{start}$, $s^{-1}$. | 650 |
| 9 | The obtained dependence $P(V) = f(V)$, from **Tables 2.3**, **2.4** | $P(V) = 85042 \cdot V^{-0.882}$ |
| 10 | Kinetic energy of the projectile, $E_{kin} = 1/2 m v_{start}^2$, J | $1.96 \cdot 10^7$ |
| 11 | Rotational energy of the projectile $E_{rot} = 1/2 (D/2)^2 m w_{start}^2$, J | $5.6 \cdot 10^4$ |
| 12 | Integration limits: $V$ – internal volume of the barrel, $V^*$ – volume of the propellant gases at atmospheric pressure, $m^3$ | 0.148; 411 |
| 13 | Work of gas expansion $E_g = \int 85042 V^{-0.882} dV$, J | $8.9 \cdot 10^5$ |
| 14 | Charge mass, $m_c$, kg | 18.4 |
| 15 | Specific explosion energy of the charge, $Q_{expl}$, J/kg | $3.6 \cdot 10^6$ |
| 16 | Energy of the charge used to fire the projectile, $E_{charge} = m_c Q_{expl}$, J | $6.62 \cdot 10^7$ |
| 17 | Energetic efficiency of the artillery gun, $eff = (E_{kin} + E_{rot} + E_g) / E_{charge}$ | 0.31 |

## 2.6 Method for verifying the impact coordinate of an artillery projectile on a surface

Studies in the field of automated control systems have demonstrated the possibility of performing automated diagnostics of the system "effective shot – projectile – flight trajectory – impact with the surface" based on the velocity of a projectile moving along a free trajectory [23–28].

This verification method can be considered as the final stage in the operation of modern automated artillery fire control systems, which rely on continuous monitoring of the states of the artillery system: "charge – breech – barrel – projectile – flight trajectory – impact with the surface".

The method is based on the task of determining the impact coordinate of an artillery projectile on a surface through acoustic registration of the sound field generated by the projectile moving along a free trajectory after being fired from an artillery gun (**Fig. 2.7**).

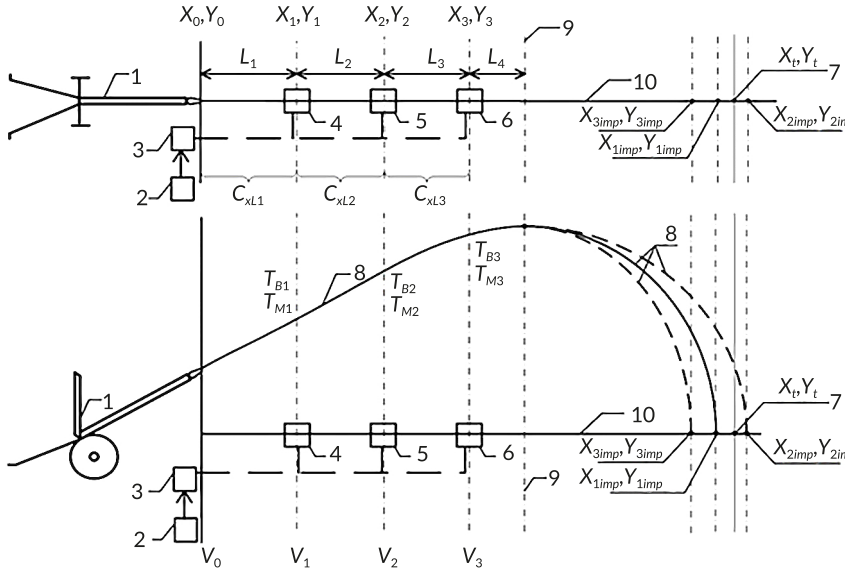


**Fig. 2.7** Layout of equipment (top and side views)

Implementation of the proposed method is carried out in the following sequence:

**Step 1**. Place the artillery gun (1), the meteorological measurement station (2), and the computing device (3). Obtain the coordinates of the gun (1) ($X_0$, $Y_0$) and the target (7) ($X_t$, $Y_t$), and enter them into the computing device (3).

**Step 2**. Along the firing line from the gun (1) to the expected table range (9), position the measuring microphones (4), (5), (6), which are connected to the computing device (3). The placement is determined by ensuring equal distances: from the gun to

the first group $L_1$, between the groups $L_2$ and $L_3$, and from the last group to the point where the projectile loses supersonic speed $L_4$.

**Step 3**. Record the coordinates of the measuring microphones (4), (5), (6) along the firing line as $(X_1, Y_1)$, $(X_2, Y_2)$, $(X_3, Y_3)$.

**Step 4**. Connect the measuring microphones (4), (5), (6) to the computing device (3) through switching equipment, synchronize them in time, and input the meteorological data (2).

**Step 5**. Fire the gun (1), causing the projectile to move along the trajectory (8) toward the target (7) at coordinates $(X_t, Y_t)$. As the projectile travels over the firing line (10), an acoustic field is formed, consisting of ballistic and muzzle waves. Both waves are recorded by the measuring microphones (4), (5), (6). The ballistic wave propagates at supersonic speed, gradually decreasing, while the muzzle wave propagates at the constant speed of sound.

**Step 6**. Each measuring microphone (4), (5), (6) first records the ballistic wave – $(T_{B1}, T_{B2}, T_{B3})$, and then the muzzle wave $(T_{M1}, T_{M2}, T_{M3})$.

**Step 7**. Calculate the time interval between the events of recording the ballistic and muzzle waves by the microphones (4), (5), (6) that are closest and farthest from the gun.

**Step 8**. Using the moments of registration of the muzzle $(T_{M1}, T_{M2}, T_{M3})$ and ballistic $(T_{B1}, T_{B2}, T_{B3})$ waves by the microphones (4), (5), (6), determine the ballistic wave velocities $(V_1, V_2, V_3)$. These values correspond to the current speed of the projectile at the moments the ballistic wave passes over the respective microphones.

**Step 9**. Determine the initial projectile velocity $V_0$ from the firing tables for the given type of charge.

**Step 10**. Calculate the drag coefficient of the projectile $(C_x)$ between the two nearest groups of microphones.

The integral drag coefficient of the projectile over the monitored section is determined by the expression

$$C_x = 2F_{ff} / (M \cdot S \cdot p \cdot V^2),$$

where $F_{ff}$ – friction force acting on the projectile of mass mmm with air over the monitored section; $S$ – cross-sectional area at the projectile's midsection; $\rho$ – air density; $V$ – average projectile velocity over the section between the two measurement points; $M$ – Mach number.

The impulse of the force is determined for two different measurement points, for example, the first (indices $i$) and the second (indices $j$). For the first point: $F_i t_i = mV_i$, hence $F_i = mV_i/t_i$, and for the second point: $F_j t_j = mV_j$, hence $F_j = mV_j / t_j$ and $V_j$ are

the current velocities of the projectile over the measurement points. $t_i$ and $t_j$ are the times of projectile travel from the gun (1) to the measurement points. Then the friction force is $F_{ff} = F_i - F_j$.

**Step 11**. Determine the trajectory approximation coefficients for the position coordinates (based on velocity, time, and trajectory length): artillery gun (1) – $a_1$, first measuring microphone or first group of microphones with switching equipment (4) – $a_2$, second measuring microphone or second group of microphones with switching equipment (5) – $a_3$, third measuring microphone or third group of microphones with switching equipment (6) – $a_4$.

**Step 12**. Construct three approximating parabolic dependencies based on the measured parameters.

The first-type parabola is formed using the coordinates of the gun (1) $X_0$ and the coordinates of the first $X_1$ and second $X_2$ microphone groups, using the trajectory coefficients $a_1$, $a_2$, $a_3$. From this dependency, the projectile-surface impact coordinate $X_{1imp}$ is determined.

The second-type parabola is formed using the coordinates of the gun $X_0$ and the first $X_1$ and third $X_3$ microphone groups, using coefficients $a_1$, $a_2$, $a_4$. From this dependency, the coordinate $X_{2imp}$ is determined.

The third-type parabola is formed using the coordinates of the gun $X_0$ and the second $X_2$ and third $X_3$ microphone groups, using coefficients $a_1$, $a_3$, $a_4$. The coordinate $X_{3imp}$ is determined from this dependency.

**Step 13.** The lateral deviation coordinates ($Y_{1imp}$, $Y_{2imp}$, $Y_{3imp}$) caused by the rotational motion of the projectile (derivation) are determined for the three parabolic dependencies.

**Step 14**. Calculate the arithmetic mean of the three projectile-surface impact coordinates ($X_{1imp}$, $Y_{1imp}$), ($X_{2imp}$, $Y_{2imp}$), and ($X_{3imp}$, $Y_{3imp}$), which represents the projectile impact location according to the proposed method.

The use of parabolic approximation in the proposed method is justified for trajectory segments where the projectile motion can be considered smooth and weakly perturbed. Under conditions of significant meteorological disturbances, complex terrain, or non-standard variations in projectile velocity along the observation segment, the approximation accuracy may decrease. In such cases, refinement of the approximation model or the use of additional measurement points may be required.

**Tables 2.6**, **2.7** present the calculation results illustrating the application of the method for determining the projectile-surface impact coordinate based on the acoustic registration of the sound field generated by the ballistic and muzzle waves.

**Table 2.6 Determination of the approximation parabola coefficients**

| Name of the parameter being determined | | Parameter values for the microphone number along the firing line | | |
|---|---|---|---|---|
| | | 1 | 2 | 3 |
| Distance to the target, km | | | 15 | |
| Distance from the gun to the microphone ($L$), m | | 5436 | 7789 | 9896 |
| Projectile velocity at the measurement point, m/s | | 674.2 | 583.3 | 519.4 |
| Length of the projectile trajectory to the measurement point, m | | 7111 | 10188 | 12944 |
| Ballistic wave registration time, s | | 10 | 15 | 20 |
| Muzzle blast wave registration time, s | | 16.4 | 23.5 | 29.8 |
| Time interval between ballistic and muzzle blast wave registrations, s | | 6.4 | 8.5 | 9.8 |
| Integral drag coefficient over the section | | 0.025940 | 0.016011 | 0.010749 |
| Approximation parabola coefficients $y = A \cdot L^2 + B \cdot L$ | $A$ | –0.000096 | –0.000088 | –0.00008 |
| | $B$ | 1.3182 | 1.2772 | 1.1937 |

**Table 2.7 Determination of the projectile-surface impact coordinate**

| Name of the parameter being determined | Parameters corresponding to the coefficients of the approximating parabola | | |
|---|---|---|---|
| | **–0.000096** | **–0.000088** | **–0.00008** |
| | **1.3182** | **1.2772** | **1.1937** |
| Calculated coordinates of the projectile impact with the surface, m | 13794 | 14511 | 15001 |
| Lateral deviation coordinates | 29 | 33 | 36 |
| Average impact coordinates of the projectile, m | | (14435; 33) | |

## 2.7 Conclusions

The results of the study allow the following conclusions to be drawn.

The main links in the chain of states "charge – chamber – barrel – projectile – flight trajectory – impact with the surface" have been identified, which characterize the life cycle of an artillery shot.

The possibility of informational localization of individual shot states has been demonstrated based on parameters of acoustic, thermodynamic, and videometric processes accompanying the shot.

A method for verifying the explosive energy of the propellant charge has been developed, based on determining the gross formula of the propellant gas and performing a subsequent thermodynamic calculation of its energetic characteristics.

An acoustic method for localizing the initial velocity of the artillery projectile based on the parameters of ballistic and muzzle waves has been proposed.

A method for determining the energetic efficiency of an artillery gun has been developed, relying on videometric registration of the projectile's exit from the barrel and the expansion of propellant gases.

A method for verifying the coordinates of the projectile's impact with the surface has been proposed, based on the analysis of the shot's acoustic fields.

**Conflict of interest**

The authors declare that they have no conflict of interest in relation to this research, whether financial, personal, authorship or otherwise, that could affect the research and its results presented in this paper.

**Use of artificial intelligence statement**

Artificial intelligence technology was used in the preparation of this chapter. Specifically, the authors used OpenAI ChatGPT (model GPT-5.2) to assist in editing and structuring introductory text sections and in formulating generalized descriptions of research methodologies for integrating mandatory literature sources into the chapter introduction.

The authors bear full responsibility for the final manuscript. Generative AI tools are not credited and are not responsible for the final results.

**Authors' contributions**

**Maksym Maksymov**: Conceptualization, Methodology, Development of models and methods, Formal analysis, Writing – original draft.

**Pavlo Gultsov**: Methodology, Investigation, Data analysis, Writing – review & editing.

**Volodymyr Demydenko**: Investigation, Validation, Interpretation of results, Writing – review & editing.

**Valentin Davydov**: Formal analysis, Visualization, Data curation, Writing – review & editing.

## References


1. Boltenkov, V., Brunetkin, O., Dobrynin, Y., Maksymova, O., Kuzmenko, V., Gultsov, P. et al. (2021). Devising a method for improving the efficiency of artillery shooting based on the Markov model. Eastern-European Journal of Enterprise Technologies, 6 (3 (114)), 6–17. https://doi.org/10.15587/1729-4061.2021.245854
2. Dobrynin, Y., Volkov, V., Maksymov, M., Boltenkov, V. (2020). Development of physical models for the formation of acoustic waves at artillery shots and study of the possibility of separate registration of waves of various types. Eastern-European Journal of Enterprise Technologies, 4 (5 (106)), 6–15. https://doi.org/10.15587/1729-4061.2020.209847
3. Dobrynin, Y., Brunetkin, O., Maksymov, M., Maksymov, O. (2020). Constructing a method for solving the riccati equations to describe objects parameters in an analytical form. Eastern-European Journal of Enterprise Technologies, 3 (4 (105)), 20–26. https://doi.org/10.15587/1729-4061.2020.205107
4. Brunetkin, O., Beglov, K., Brunetkin, V., Maksymov, O., Maksymova, O., Havaliukh, O. et al. (2020). Construction of a method for representing an approximation model of an object as a set of linear differential models. Eastern-European Journal of Enterprise Technologies, 6 (2 (108)), 66–73. https://doi.org/10.15587/1729-4061.2020.220326
5. Brunetkin, O., Maksymov, M., Brunetkin, V., Maksymov, O., Dobrynin, Y., Kuzmenko, V. et al. (2021). Development of the model and the method for determining the influence of the temperature of gunpowder gases in the gun barrel for explaining visualize of free carbon at shot. Eastern-European Journal of Enterprise Technologies, 4 (1 (112)), 41–53. https://doi.org/10.15587/1729-4061.2021.239150
6. Brunetkin, O., Maksymov, M., Dobrynin, Y., Demydenko, V., Sidelnykov, O. (2024). Development of a process model for determining the composition and energy characteristics of a pyrotechnic mixture using the library method. EUREKA: Physics and Engineering, 5, 99–112. https://doi.org/10.21303/2461-4262.2024.003453
7. Brunetkin, O., Dobrynin, Y., Maksymenko, A., Maksymova, O., Alyokhina, S. (2020). Inverse problem of the composition determination of combustion products for gaseous hydrocarbon fuel. Computational Thermal Sciences:

An International Journal, 12 (6), 477–489. https://doi.org/10.1615/computthermalscien.2020034878
8. Maksymov, M. V., Brunetkin, O. I., Beglov, K. V., Alyokhina, S. V., Butenko, O. V. (2022). Automatic Control for the Slow Pyrolysis of Organic Materials with Variable Composition. Advanced Control Systems. River Publishers, 397–434. https://doi.org/10.1201/9781003337010-16
9. Brunetkin, A., Beglov, K., Maksimov, M. Ulitskaja, E. (2021). Model and method of controlled pyrolysis of organic sub-stances of variable composition. International Scientific Technical Journal "Problems of Control and Informatics", 66 (1), 134–146. https://doi.org/10.34229/1028-0979-2021-1-12
10. Brunetkin, O., Sidelnykov, O., Maksymov, M., Dobrynin, Y. (2025). Improving the model for determining the composition of gunpowder gases during thermal destruction of gunpowder in a limited volume space. Eastern-European Journal of Enterprise Technologies, 3 (6 (135)), 35–45. https://doi.org/10.15587/1729-4061.2025.330654
11. Katsev, I. (2018). Evaluation method of the artillery's effectiveness against unitary target. International Scientific Journal "Security & Future", 2 (4), 196–198. Available at: https://stumejournals.com/journals/confsec/2018/4/196.full.pdf
12. Field Manual 3-09 Field Artillery Operations and Fire Support (2014). Washington: Department of the Army, 4–12. Available at: https://www.scribd.com/document/248059115/FM-3-09-Field-Artillery-Operations-and-Fire-Support
13. ADLER II Artillery Computer Network Delivered to Troops. Army Technology. Available at: https://www.army-technology.com/contractors/data/kulr-technology-partners-us-army/pressreleases/press15/
14. Field Manual 3-09.22 Tactics, Techniques, and Procedures for Corps Artillery, Division Artillery, and Field Artillery Brigade Operations (2001). Washington: Department of the Army. Available at: https://www.globalsecurity.org/military/library/policy/army/fm/3-09-22/index.html
15. Dobrynin, Y., Maksymov, M., Boltenkov, V. (2020). Development of a method for determining the wear of artillery barrels by acoustic fields of shots. Eastern-European Journal of Enterprise Technologies, 3 (5 (105)), 6–18. https://doi.org/10.15587/1729-4061.2020.206114
16. Dobrynin, Ye., Davydov, V. (2020). Simulation model of the information technology for the technical diagnosis of the impulse heat machine. Odes'kyi Politechnichnyi Universytet Pratsi, 2 (61), 95–103. https://doi.org/10.15276/opu.2.61.2020.11
17. Dobrynin, Y. V., Boltenkov, V. O., Maksymov, M. V. (2020). Information technology for automated assessment of the artillery barrels wear based on SVM

classifier. Applied Aspects of Information Technology, 3 (3), 117–132. https://doi.org/10.15276/aait.03.2020.1
18. Tkachyk, P. P., Budaretskiy, Y. I., Shchavinskiy, Y. V., Prokopenko, V. V. (2015). Influence of automation control units and artillery fire on the effectiveness of its application. Military Technical Collection, 12, 75–82. https://doi.org/10.33577/2312-4458.12.2015.75-82
19. Maksymov, M. V., Brunetkin, O. I., Lysiuk, O. V., Tarakhtii, O. S. (2019). Pat. No. 120216 UA. Ustanovka dlia vyznachennia skladu horiuchoho hazu pry yoho spaliuvanni. No. a201712785; declareted: 22.12.2017; published: 25.10.2019, Bul. No. 20.
20. Brunetkin, O., Dobrynin, Y., Maksymenko, A., Maksymova, O., Alyokhina, S. (2020). Model and method of conditional formula determination of oxygen-containing hydrocarbon fuel in combustion. Energetika, 66 (1). https://doi.org/10.6001/energetika.v66i1.4298
21. Dobrynin, Y. V., Boltenkov, V. O., Kuzmenko, V. V., Maksymov, O. M. (2022). Development of a universal binary classifier of the state of artillery barrels by the physical fields of shots. Applied Aspects of Information Technology, 5 (4), 289–302. https://doi.org/10.15276/aait.05.2022.19
22. Brunetkin, O., Kuzmenko, V., Soloviova, O. (2022). Mathematical model of energy transformation processes in barrel system for determining shooting performance. Energy Engineering and Control Systems, 8 (1), 28–39. https://doi.org/10.23939/jeecs2022.01.028
23. Maksymov, M. V., Boltenkov, V. O., Gultsov, P. S., Maksymov, O. M. (2023). Verification of artillery fire under the influence of random disturbances for the computer game ARMA 3. Applied Aspects of Information Technology, 6 (4), 362–375. https://doi.org/10.15276/aait.06.2023.24
24. Maksymova, O. B., Boltenkov, V. O., Maksymov, M. V., Gultsov, P. S., Maksymov, O. M. (2023). Development and optimization of simulation models and methods for controlling virtual artillery units in game scenarios. Herald of Advanced Information Technology, 6 (4), 320–337. https://doi.org/10.15276/hait.06.2023.21
25. Maksymova, O., Boltyonkov, V., Gultsov, P., Maksymov, O. (2023). Improvement of the model and method of artillery installation target damage control with minimal combat capability loss. Odes'kyi Politechnichnyi Universytet Pratsi, 2 (68), 98–115. https://doi.org/10.15276/opu.2.68.2023.11
26. Maksymov, M. V., Hultsov, P. S., Boltyonkov, V. O., Maksymov, O. M. (2024). Method for verification of artillery firing under the influence of random disturbances. Maritime Security and Defense, 1, 36–49. https://doi.org/10.32782/msd/2024.1/05

27. Tarakhtiy, O. S., Gultsov, P. S., Maksymov, O. M. (2024). Udoskonalennia metodu i modeli keruvannia boiovoiu zdatnistiu artyleriiskoi harmaty. Proceedings of the 5th International Scientific and Practical Conference. Tokyo: CPN Publishing Group, 256–261. Available at: https://sci-conf.com.ua/v-mizhnarodna-naukovo-praktichna-konferentsiya-topical-aspects-of-modern-scientific-research-25-27-01-2024-tokio-yaponiya-arhiv
28. Tarakhtiy, O. S., Hultsov, P. S., Maksymov, O. M. (2024). Udoskonalennia metodu i modeli keruvannia boiovoiu zdatnisttiu artyleriiskoi harmaty. European Congress of Scientific Achievements. Proceedings of the 1st International Scientific and Practical Conference. Barcelona: Barca Academy Publishing, 120–125. Available at: https://sci-conf.com.ua/wp-content/uploads/2024/01/EUROPEAN-CONGRESS-OF-SCIENTIFIC-ACHIEVEMENTS-29-31.01.24.pdf